

# IMPLEMENTATION OF NEW SOURCE TERMS IN A THIRD GENERATION WAVE MODEL

Jean-Michel Lefèvre  
Météo-France, Toulouse, France

Simona Ecaterina Ștefănescu  
National Meteorological Administration, Bucharest, Romania

Vladimir Makin  
Royal Netherlands Meteorological Institute, De Bilt, The Netherlands

## 1. INTRODUCTION

In a recent study (Lefevre et al., 2003; Ștefănescu et al., 2004), performances of three wave models have been assessed. VAG (Guillaume 1987, Fradon et al. 2000, Ștefănescu and Lefvre 2001) WAM (Komen et al., 1994), WAVEWATECH III (referred to as WW3, Tolman and Chalikov, 1996, Tolman 2002) have been run with same wind forcings and results were compared to buoys data. It has been found that VAG and WAM are underpredicting high swell systems (often, wind sea and swell are mixed in these cases) while WW3 performs very well. Investigations indicated that sources terms were responsible for such discrepancies. In small to moderate fetch conditions (up to typically 400 km) WAM and WW3 underpredict wave height by about 15 percent in winter. For smaller fetch (up to 100 km), the underprediction is even larger for WW3. The underprediction could be reduced in WW3 by tacking into account air-sea temperature stability conditions (Tolman, personal communication). These results are in agreement with Banner and Young (1994) where the dissipation formulation is believed to be responsible for a too small dissipation rate at the spectral peak during young sea growth and a too strong dissipation rate for old wind seas. Moreover the WAM (and VAG) dissipation formulation as it is implemented in WAM and VAG is very sensitive on the occurrence of swell or wind sea in mixed sea-swell situations. After the wind-over-waves coupling theory (WOWC) introduced by Janssen (1989, 1991) associated with an air-sea coupling formulation implemented in WAM cycle 4, a modern WOWC theory was recently developed by Makin et al. (1995), Makin and Kudryavtsev (1999), Kudryavtsev and Makin (1999), Kudryavtsev and Makin (2001) and Makin and Kudryavtsev (2002). This theory includes a physical model for short waves, based on the energy balance equation, and accounts for stress due to the Air Flow Separation (AFS) from short

and dominant waves and also for the wave-induced stress. The parameterization of the surface stress (sea drag) is based on this theory and its implementation in the NEDWAM model (the North Sea version of the WAM model) is described in Makin and Stam (2003). The parameterization accounts for the wind speed, wave age and finite bottom dependencies of the surface stress. The sensitivity study presented in Makin and Stam (2003) has shown that the NEDWAM model is not sensitive to the parameterization of the sea drag and, for this reason, new formulations of wind input and dissipation due to the wave breaking, based on the new understanding of physics of the processes, have been implemented. The new formulations implemented in NEDWAM have been calibrated and tested in the North Sea where shallow water conditions prevail, so there is a need for an assessment in a global wave model, with deep water conditions. In the present study, the new parameterization of the sea drag, as well as the new formulations of wind input and dissipation source terms, have been implemented in WAM (as in NEDWAM) and tested on a global grid at a spatial resolution of  $1^\circ \times 1^\circ$ . The new physics introduced in the WAM model have been tested during an intercomparison study of the performance of three ocean wave models with moored buoy data. For the experiments, two periods of 1 month were selected: one winter month of February 2002 and one summer month of July 2002. Sensitivity experiments with VAG, WAM, and WW3 models have been carried out using available analysed 10 m wind field from the global operational numerical weather prediction (NWP) models of ECMWF (IFS - Simmons et al., 1989). The results were compared against buoy data. The new formulations of sea drag and wind input and dissipation source terms introduced in the WAM model resulted in a better prediction of significant wave height (swH) in many cases and reductions in the bias and rms error of this parameter.

The paper is organized as follows. Section 2

gives a short description of the new sea drag and wind input and dissipation source terms formulations introduced in the WAM model are discussed. Section 3 presents the three ocean wave models and buoy data used in this study. Sensitivity experiments with VAG and WAM models and comparison of the results with buoy and model data are included in section 4. Conclusions and perspectives are pointed out in section 5.

## 2. NEW INPUT SOURCE TERMS

A new air-sea coupling formulation has been recently developed by Makin et al. (1995), Makin and Kudryavtsev (1999), Kudryavtsev and Makin (1999), Kudryavtsev and Makin (2001) and Makin and Kudryavtsev (2002). Its implementation and testing in the NEDWAM model is presented in Makin and Stam (2003). The new parameterization is valid only under stationary and spatial homogeneous wind and waves conditions, when the constant-flux layer is established in the marine atmospheric surface boundary layer. It can be applied for both pure windsea and mixed windsea-swell conditions. However, only the windsea part of the wave spectrum is used to calculate the sea drag, while the contribution of swell spectrum is not accounted for. Therefore, the parameterization assumes that the wind waves direction coincides with the wind direction.

The third generation wave model WAM solves explicitly (without any assumptions on the shape of the wave spectrum) the energy balance equation, in which the source function is defined as a superposition of four source terms: wind input, dissipation by wave breaking, bottom friction dissipation and non-linear interactions between the wave components. The source terms of the WAM model cycle 4 (referred to as WAM4) are described in WAMDIG (1988), Günther et al. (1992) and Komen et al. (1994).

The sensitivity study presented in Makin and Stam (2003) showed that the NEDWAM model is not sensitive to the parameterization of the sea drag and, for this reason, new formulations of wind input and dissipation due to the wave breaking, based on the new understanding of physics of the processes, were implemented.

The quasi-linear form of the dissipation source term  $S_{dis}$  used in the WAM4:

$$S_{dis} = \gamma_{dis} \omega F \quad (1)$$

is defined in terms of the integrated spectral steepness, as proposed by Hasselmann (1974). The dis-

sipation rate  $\gamma_{dis}$  reads:

$$\gamma_{dis} = -C_{dis} \frac{\langle \omega \rangle}{\omega} \left( \frac{\alpha}{\alpha_{PM}} \right)^2 \frac{k}{2\langle k \rangle} \left( 1 + \frac{k}{\langle k \rangle} \right) \quad (2)$$

where  $k$  is the wavenumber,  $\alpha_{PM} = 4.57 \times 10^{-3}$  is the Pierson-Moskowitz steepness for a fully developed sea,  $\alpha = E\langle k \rangle^2$  is the squared average steepness of the spectrum and  $C_{dis} = 9.4 \times 10^{-5}$  is a dimensionless constant.  $E$  represents the total wave variance, while  $\langle \omega \rangle$  and  $\langle k \rangle$  are the mean angular frequency and mean wavenumber.

Formulation (3) gives a dissipation rate at the spectral peak that is too low during young wind-sea growth and too strong for old windseas (Banner and Young 1994, Makin and Stam 2003). It is based on the average wave steepness, which is not appropriate for mixed windsea-swell situations.

A new spectral dissipation source term, based on the local wave steepness and strongly non-linear dependent of the wave spectrum, has been suggested by Alves and Banner (2003). This new formulation improves the prediction of wave evolution from young to old seas, in accordance with field observations. Alves and Banner (2003) proposed the following expression for the dissipation rate:

$$\gamma_{dis} = -C_{dis}^b \left( \frac{\alpha}{\alpha_{PM}} \right)^m \left( \frac{B(k)}{B_r} \right)^{p/2} \left( \frac{k}{\langle k \rangle} \right)^n \quad (3)$$

where  $C_{dis}^b$ ,  $m$ ,  $p$ ,  $n$  and  $B_r$  are constants (to be adjusted for the new balance), and  $B(k)$  is the saturation wave spectrum related to the wave density spectrum  $F(f)$  by:

$$B(k) = \frac{1}{2\pi} F(f) c_g k^3 \quad (4)$$

where  $c_g$  is the group velocity.

The dissipation source function  $S_{dis} = \gamma_{dis} \omega F$  is now non-linear with respect to  $F$ , as the spectrum  $B(k)$  (or  $F(f)$ ) enters directly in the dissipation rate.

The parameterization of the wind input used in WAM model cycle 4 is based on the quasi-laminar critical layer model of the airflow developed by Miles (1957, 1959). Kudryavtsev et al. (1999) showed that the applicability of the quasi-laminar model in the description of the airflow dynamics is very limited. Usually, the wind input source function  $S_{in}$  is written as follows:

$$S_{in} = \beta \omega F \quad (5)$$

where  $\beta$  is the growth rate parameter. Makin et al. (1999) suggested an alternative formulation for the

growth rate parameter:

$$\beta = \frac{\rho_a}{\rho_w} m_\beta R \left(\frac{u_*}{c}\right)^2 \cos(\theta - \theta_w) |\cos(\theta - \theta_w)| \quad (6)$$

where  $\rho_a$  and  $\rho_w$  are the density of air and water and  $m_\beta$  is a constant. Function  $R$  is defined by:

$$R = 1 - m_c \left(\frac{c}{u_{10}}\right)^{n_c} \quad (7)$$

$R$  has values close to 1 for slowly moving waves and negative values for fast moving waves. Notice, that the wind input source term will be negative for fast moving waves or (and) waves traveling in the opposite direction relative to wind direction.

The new balance was tuned for the NEDWAM model in the North Sea region, for shallow water conditions, yielding the following constants:  $C_{dis}^b = 2.5 \times 10^{-5}$ ,  $B_r = 4 \times 10^{-3}$ ,  $m = 2$ ,  $p = 6$  and  $n = 1$  for the dissipation source term and  $m_\beta = 0.045$ ,  $m_c = 0.3$  and  $n_c = 5$  for the wind input source term. The proportionality coefficient for the bottom friction source term  $S_{bot}$  was tuned to twice the original value (from 0.076 to 0.152), without changing the bottom friction source term formulation.

### 3. DESCRIPTION OF THE MODELS AND BUOY DATA

#### a. Buoy data and Wind forcing

The buoy data consist of wind speed and direction, swh and mean (only for the buoys located in the west coast of Europe) or peak wave period. Buoy peak period can not be compared with model mean period, but it is useful to distinguish which kind of waves occur (windsea, swell or mixed windsea-swell). The buoy measurements have been averaged over periods of 4 hours and are available at a 6h interval. The wind speed and direction at the buoy location were not adjusted to the 10 m level. Data from 30 moored buoys were used in this study. Only 2 buoys (44011 and 63111) are located in shallow water regions, while the rest of them are located in deep water regions. Figure 1 shows the locations of the buoys and table 1 presents additional information about each buoy. The five-digit WMO buoy identifier is followed by the name of buoy and the name of the region to which it belongs: Hawaii (HW), the west coast of the European continent (WCE), the west coast of the North American continent (WCNA) and the east coast of the North American continent (ECNA).

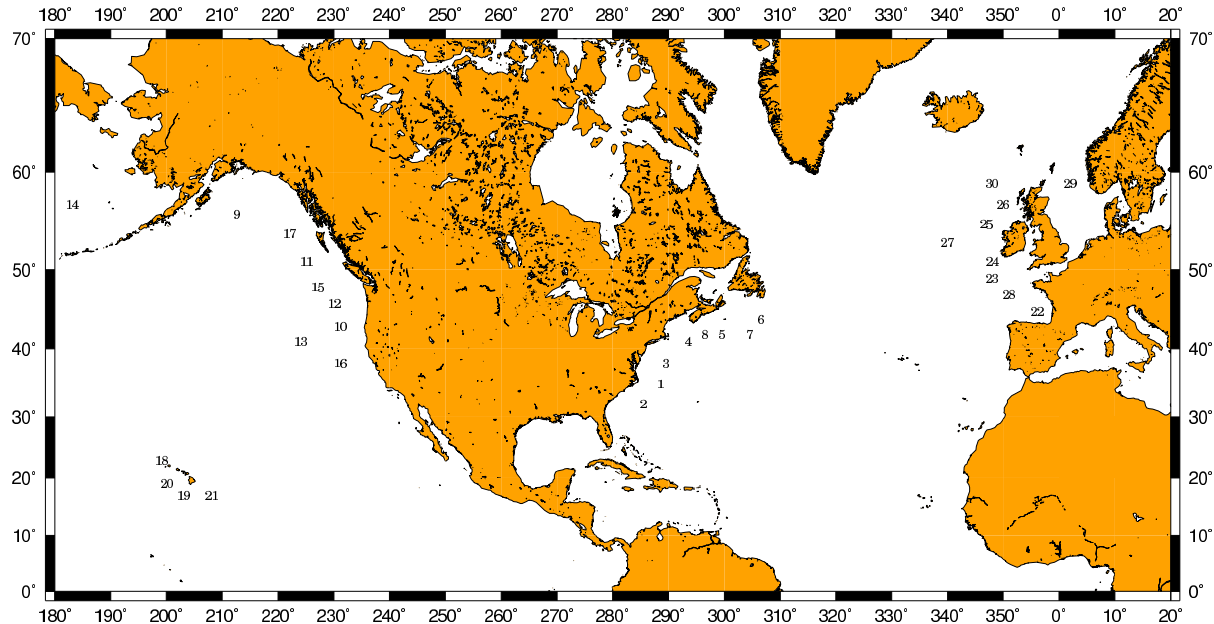


Figure 1: Locations of the buoys used in this study.

|  |  |
|--|--|
| 1 41001 US East Coast, E Hatteras ECNA         | 16 46059 US West Coast, California WCNA          |
| 2 41002 US South-East Coast, S Hatteras ECNA   | 17 46184 Canada West Coast, North Nomad WCNA     |
| 3 44004 US North-East Coast, Hotel ECNA        | 18 51001 Hawaii North-West HW                    |
| 4 44011 US North-East Coast, Georges Bank ECNA | 19 51002 Hawaii South-West HW                    |
| 5 44137 Newfoundland, East Scotia slope ECNA   | 20 51003 Hawaii West HW                          |
| 6 44138 Newfoundland, SW Grand Bank ECNA       | 21 51004 Hawaii South-East HW                    |
| 7 44141 Newfoundland, Laurentian Fan ECNA      | 22 62001 Gulf of Biscay, Gascogne WCE            |
| 8 44142 Nova Scotia, Lahave Bank ECNA          | 23 62029 UK Celtic Sea shelf break (K1) WCE      |
| 9 46001 Gulf of Alaska WCNA                    | 24 62081 UK East Atlantic (K2) WCE               |
| 10 46002 US West Coast, Oregon WCNA            | 25 62105 UK East Atlantic (K4) WCE               |
| 11 46004 Canada West Coast, Middle Nomad WCNA  | 26 62106 UK North-East Atlantic RARH WCE         |
| 12 46005 US North-West Coast, Washington WCNA  | 27 62108 UK East Atlantic (K3) WCE               |
| 13 46006 US West Coast, SE Papa WCNA           | 28 62163 UK Celtic Sea shelf break (Britany) WCE |
| 14 46035 Bering Sea                            | 29 63111 North Sea shelf break (Beryl A)         |
| 15 46036 Canada West Coast, South Nomad WCNA   | 30 64045 UK North-East Atlantic WCE              |

Table 1: The WMO buoys identifiers, names and regions to which these belongs.

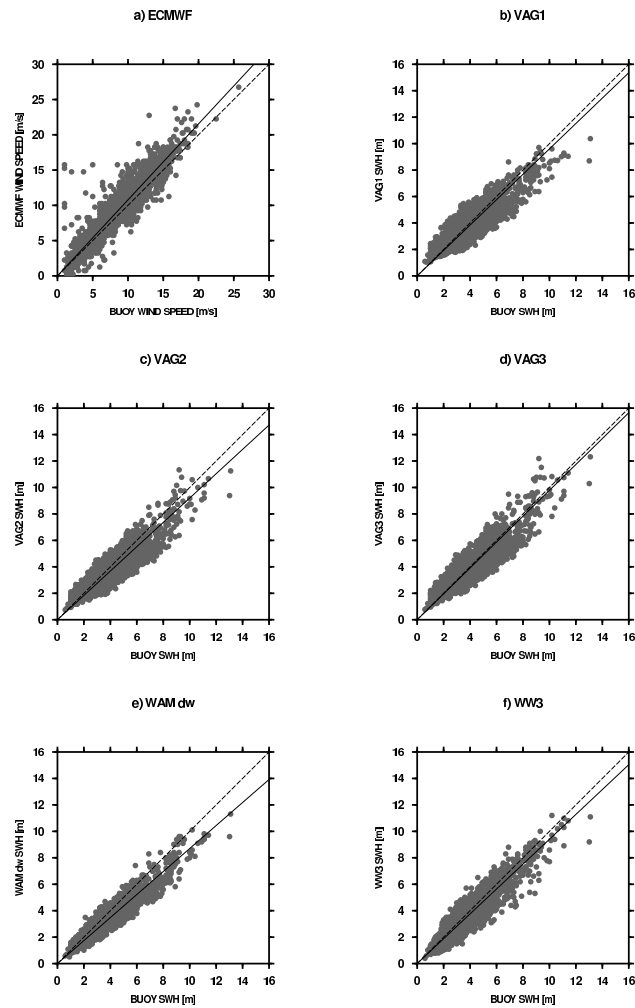


Figure 2: Comparisons of ECMWF winds with buoys data (a), and of VAG, WAM and WW3 wave heights with buoy data, for february 2002

The analysed 10 m wind field from the operational NWP models of ECMWF (IFS) were used as input for all wave models. The spatial resolution of the wind field was  $1^\circ \times 1^\circ$  for IFS model. A coupling frequency of 6h was used for all wave models. Comparisons of ECMWF winds with buoys data and of VAG, WAM and WW3 wave heights with buoy data for february 2002 are shown on figure 2. VAG1 denotes a previous version of the VAG model while VAG3 is similar to VAG2 with a different tuning of the input source terms coefficients (Stefanescu and Lefevre 2001)

#### b. Wave models

In order to assess the contribution of the wind input term and of the dissipation term separately, several configurations of WAM were considered. In *WAM\_M3*, the input source term from Makin and Kudriastsev (1999) and the WAM3 dissipation term were introduced. In WAM, only the new sea drag and wind input formulations are introduced with unchanged WAM4 dissipation term. All wave models were run on a global grid with a spatial resolution of  $1^\circ \times 1^\circ$ . The main characteristics of VAG, WAM (with different configurations) and WW3 are presented in Table 2.

| Model  | Wave physics  | Spectral discretization         | Time steps  | Source terms  |
|--------|---------------|---------------------------------|---|---|
| VAG2   | deep water    | 22 frequencies<br>18 directions | propagation: 900s<br>source terms integration: 900s                               | new physics<br>a=0.1, b=0.7, c=0.5                          |
| WW3    | deep water    | 25 frequencies<br>24 directions | global: max 3600s<br>propagation: max 1300s<br>source terms integration: min 300s | Tolman and<br>Chalikov                                      |
| WAM dw | deep water    | 25 frequencies<br>18 directions | propagation: 600s<br>source terms integration: 600s                               | sea drag: WAM 4.0<br>input: WAM 4.0<br>dissipation: WAM 4.0 |
| WAM sw | shallow water | 25 frequencies<br>18 directions | propagation: 600s<br>source terms integration: 600s                               | sea drag: WAM 4.0<br>input: WAM 4.0<br>dissipation: WAM 4.0 |
| WAM_MM | shallow water | 25 frequencies<br>18 directions | propagation: 600s<br>source terms integration: 600s                               | sea drag: Makin<br>input: Makin<br>dissipation: Makin       |
| WAM_M3 | shallow water | 25 frequencies<br>18 directions | propagation: 600s<br>source terms integration: 600s                               | sea drag: Makin<br>input: Makin<br>dissipation: WAM 3.0     |
| WAM_M4 | shallow water | 25 frequencies<br>18 directions | propagation: 600s<br>source terms integration: 600s                               | sea drag: Makin<br>input: Makin<br>dissipation: WAM 4.0     |

Table 2: The main characteristics of the wave models used in this study

#### 4. SENSITIVITY STUDY

a. Experiments made with several configurations of WAM

Different configurations of the WAM model were considered in our sensitivity study, depending on the wind input and dissipation formulations and the value of some coefficients ( $cb = \rho_w / \rho_a m_\beta R$ , used in the wind input source term, and  $p$  used in the dissipation term):

- *WAM\_MMcb* - 20p6 with  $cb = \max(-20, cb)$  and  $p = 6$ ;
- *WAM\_MMcb* - 20p0 with  $cb = \max(-20, cb)$  and  $p = 0$ ;

- *WAM\_MMcb* - 100p6 with  $cb = \max(-100, cb)$  and  $p = 6$ ;
- *WAM\_MMcb* - 20p0t6 with  $cb = \max(-20, cb)$  and  $p$  defined as a function of the ratio  $B(k)/B_r$ , as proposed by Alves and Banner (2003):

$$p = \frac{p_0}{2} + \frac{p_0}{2} \tanh\{10[(\frac{B(k)}{B_r})^{1/2} - 1]\} \quad (8)$$

with  $p_0$  a constant set up numerically to 6.

- *WAM\_M3cb* - 20 with  $cb = \max(-20, cb)$ ;
- *WAM\_M4cb* - 20 with  $cb = \max(-20, cb)$ .

Makin and Stam (2003) proposed  $cb = \max(-20, cb)$  and a constant value for  $p$ , namely 6. First experiment with *WAM\_MMcb* - 20p6

configuration showed that the swell dissipation is too small in this case (see figure 3 for buoy 46005 located in the West coast of the North American continent region, for which periods with swell situations are pointed out by the high peak period measured at the buoy). For this reason, additional experiments with the new sea drag and wind input formulations, but with dissipation taken from WAM3 or WAM4, were performed. For these experiments  $cb$  was set to  $\max(-20, cb)$ . The experiments made with  $WAM\_M4cb - 20$  showed swh values close to those obtained with the WAM4. The impact of the new wind input term is therefore small. If we set up the parameter  $p$  to 0, than the dissipation source term described by (2) and (4) will differ from the WAM3 dissipation source term only by the use of angular frequency  $\omega$  instead of the mean angular frequency  $\langle \omega \rangle$ . This should lead to a smaller dissipation of swell and a stronger dissipation of windsea by  $WAM\_MMcb - 20p0$ , compared to  $WAM\_M3cb - 20$ . The experiments showed that the results obtained with  $WAM\_MMcb - 20p0$  are rather close to that ones obtained in case of  $WAM\_M3cb - 20$ . Therefore,  $p = 0$  works well for swell dissipation, as  $WAM\_M3cb - 20$ , thought it

is not the case for WAM3. So there is an impact of Makin wind input term when WAM3 dissipation term is used, unlike with WAM4 dissipation term.

Also, Alves and Banner (2003) suggested that  $[B(k)/B_r]^{p/2}$  should approach 1 in case of spectral components with reduced local steepness, like swell. By setting  $p = 0$  we satisfy this condition and the results presented in figures 4 and 5 show a better description of swell dissipation in this case. Figure 6 shows the swh for windsea situations occurred at buoy 44141 (this buoy is located in a fetch limited area). For this buoy, a significant overestimation of the swh peaks occurs in case of setting  $p = 0$ . The dissipation is too small. For waves with large local steepness ( $B(k)/B_r > 1$ ), a constant value for  $p$  (set up to 6 in our experiments) is more appropriate, giving better results.

Using  $WAM\_MMcb - 100p6$ , the results are very good for windsea situations (see figure 7), but the swell dissipation is too strong and high swells are underpredicted(not shown) . Therefore, and as expected, it appears that it is not appropriate to use a constant value for  $p$  in case of mixed windsea-swell situations, as it was done in Mafin and Stam (2003) implementation.

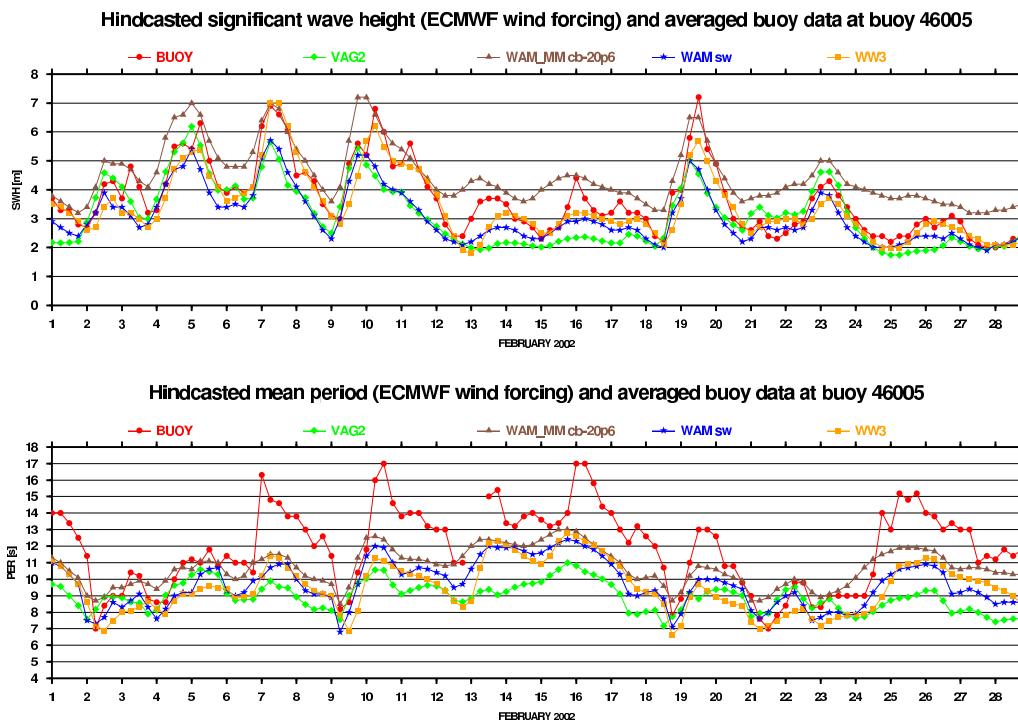


Figure 3: Time series of swh and mean (for the models) or peak (for the buoy) period at buoy 46005 for February 2002

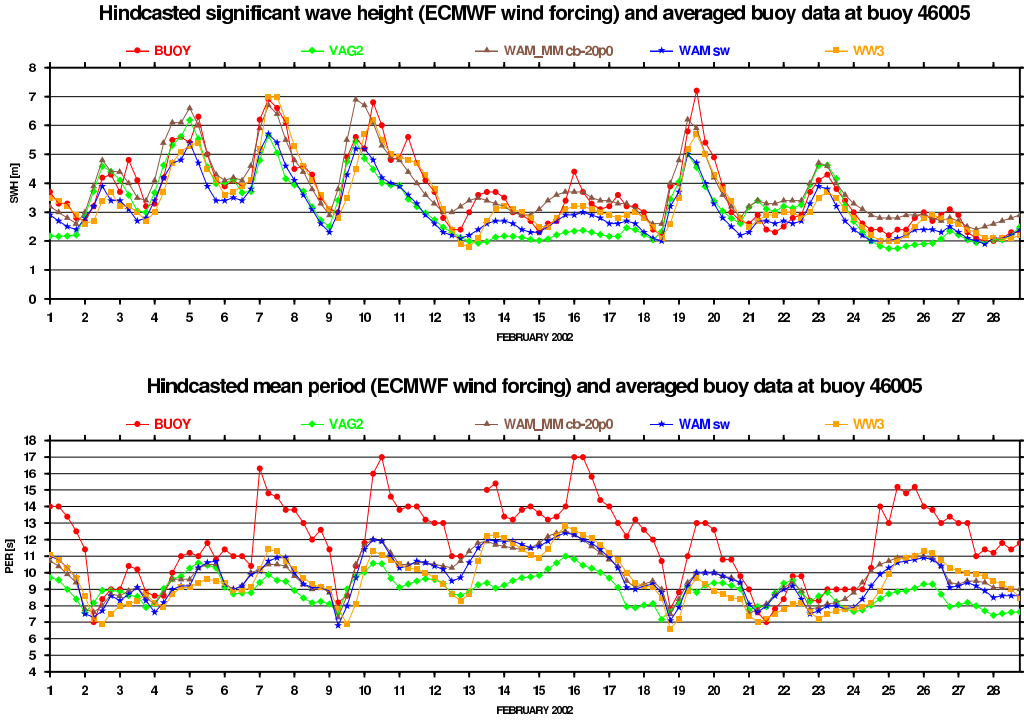


Figure 4: Time series of swh and mean (for the models) or peak (for the buoy) period at buoy 46005 for February 2002

Alves and Banner (2003) suggested to define  $p$  as in expression (9). In this case,  $p$  is equal to 0 for waves with a reduced local steepness (swells) and it takes a constant value  $p_0$  (in our case  $p_0$  is set to 6) for waves with a big local steepness (windseas). The experiments made with  $WAM\_MMcb-20p0t6$  configuration showed that the improvements in swell dissipation are still kept (see figures 8 and 9), while the overestimation of the windsea peaks is removed (figure 10).

b. Global statistics for the models used in the intercomparison study

Statistics for experiments performed with the ECMWF wind field are presented. The quality of the analysed wind speed of ECMWF is good for both February and July periods (see tables 2 and 4). Scatter diagrams (figures 11 and 12) and symmetric slopes (tables 2 and 4) indicate a small overestimation of the ECMWF wind speed data compared to the buoys data. The bias can be explained by the altitudes differences of altitude between the buoy anemometers and the 10m reference level used for model wind data. From table 3 it can be seen

that for February  $WAM\_MMcb-20p0t6$  swh has the best quality between all WAM configurations (see also scatter diagrams on figure 11). Comparing  $WAM\_MMcb-20p0t6$  statistics with statistics computed for shallow water run of WAM cycle 4 ( $WAMsw$ ), there is a clear improvement of rms error, scatter index and symmetric slope. For July, rms error and symmetric slope is better for  $WAM\_MMcb-100p6$  configuration (comparing to the other WAM configurations presented in table 5 and on figure 12). Time series also showed better agreement of  $WAM\_MMcb-100p6$  swh with buoy data. The  $WAM\_MMcb-20p0t6$  swh is overestimated for July. For the total period (February + July), the  $WAM\_MMcb-20p0t6$  configuration appears to have the best quality between all WAM configurations (not shown).

Comparing the three wave models statistics (VAG and WAM with different configurations and WW3), we can see that for February  $WAM\_MMcb-20p0t6$  swh has the best quality (it is better even than WW3 swh), while for July WW3 swh has better quality than  $WAM\_MMcb-20p0t6$  swh and comparable quality with  $WAM\_MMcb-100p6$  swh.

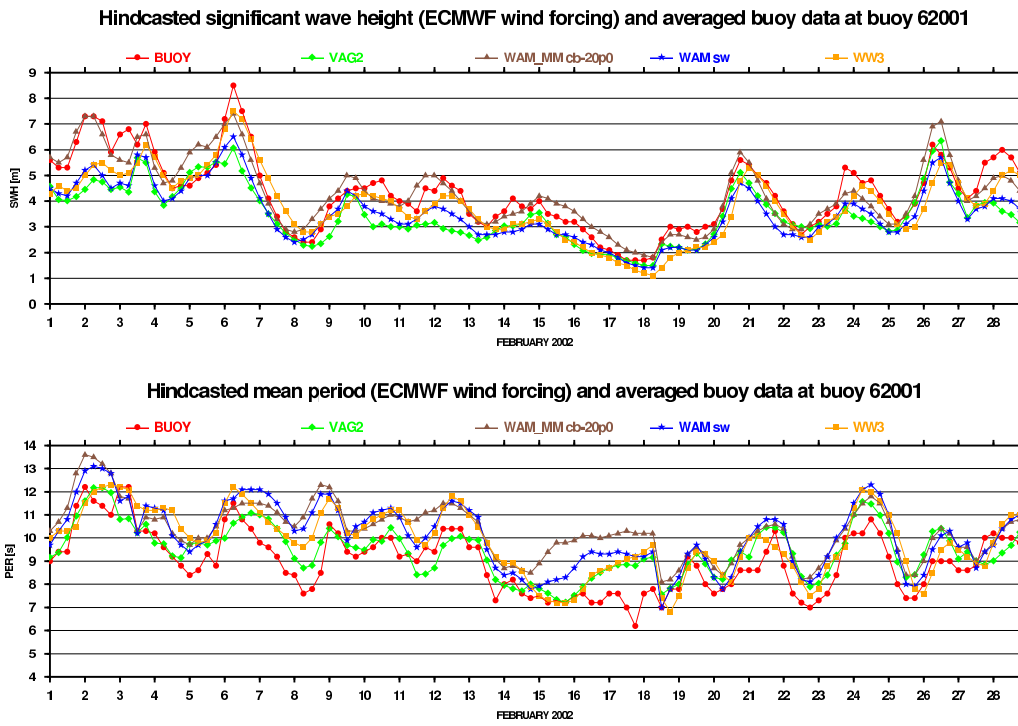


Figure 5: Time series of swh and mean period at buoy 62001 for February 2002

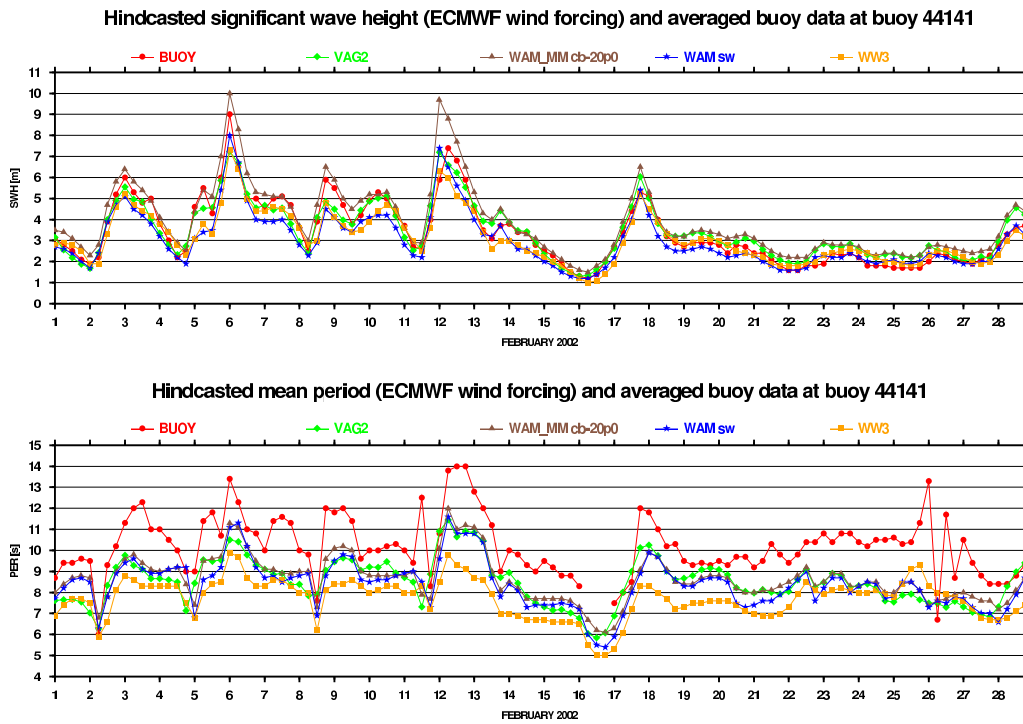


Figure 6: Time series of swh and mean (for the models) or peak (for the buoy) period at buoy 44141 for February 2002

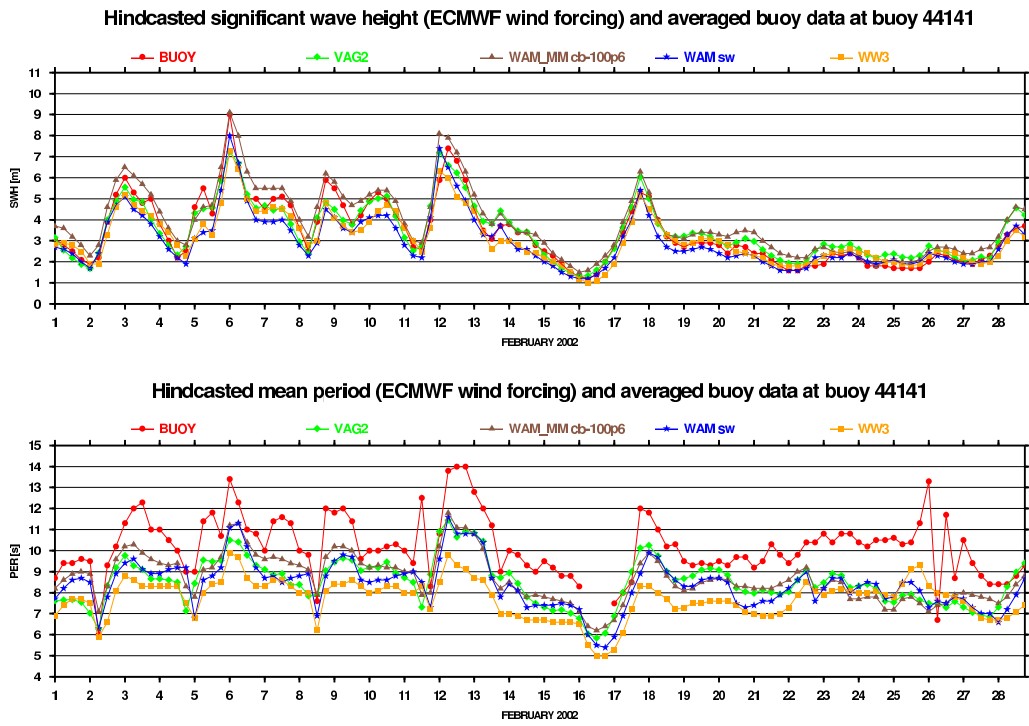


Figure 7: Time series of swh and mean (for the models) or peak (for the buoy) period at buoy 44141 for February 2002

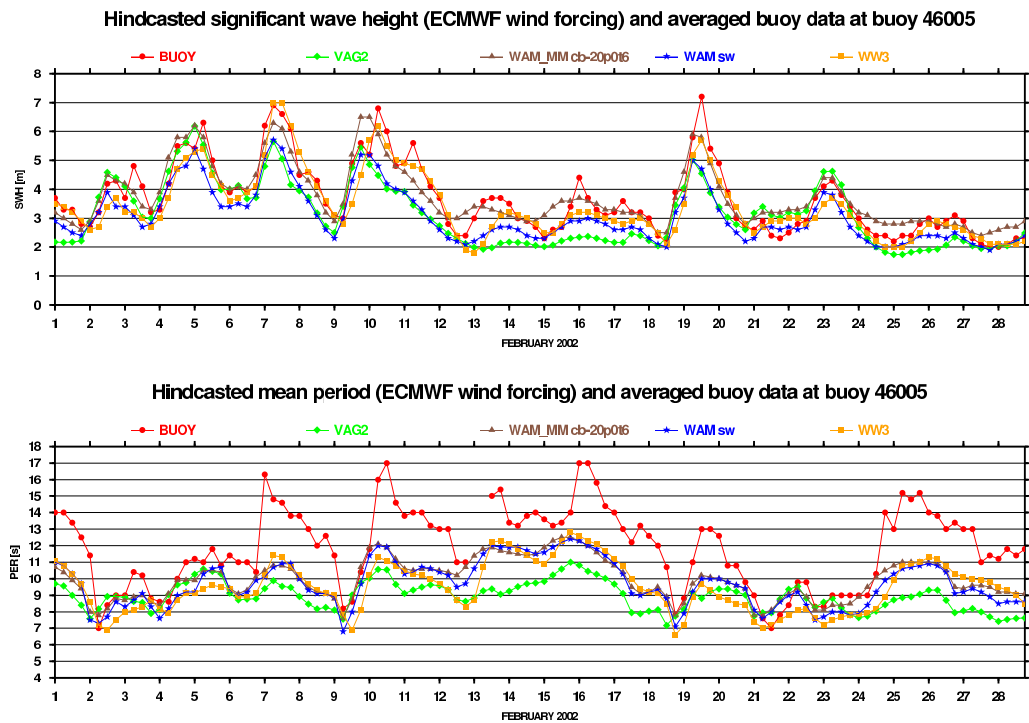


Figure 8: Time series of swh and mean (for the models) or peak (for the buoy) period at buoy 46005 for February 2002

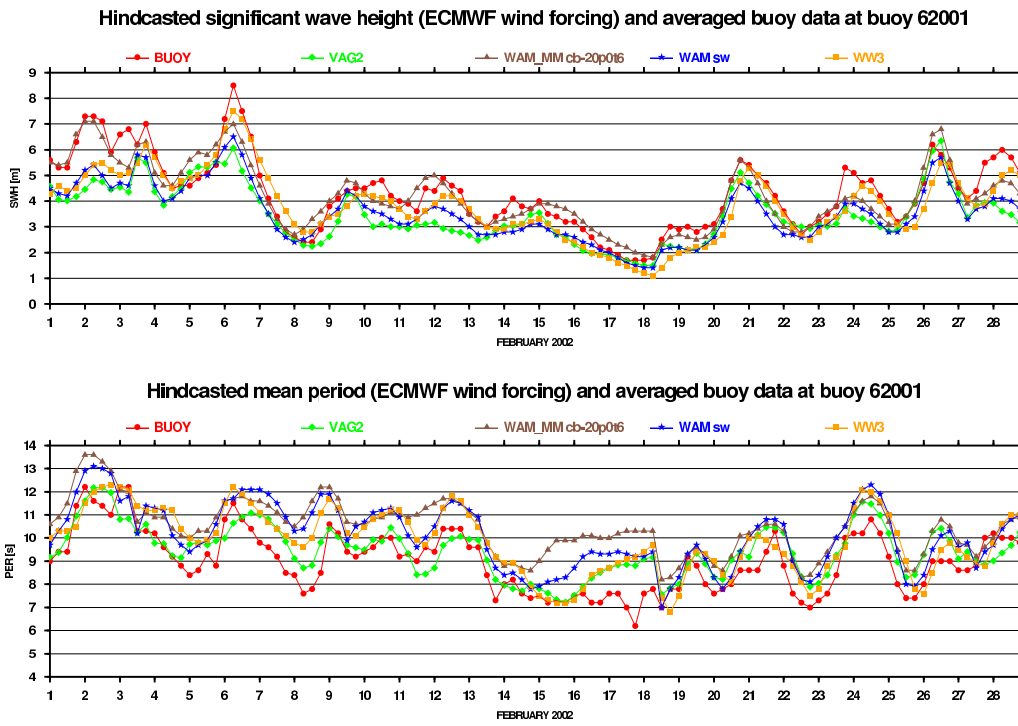


Figure 9: Time series of swh and mean period at buoy 62001 for February 2002

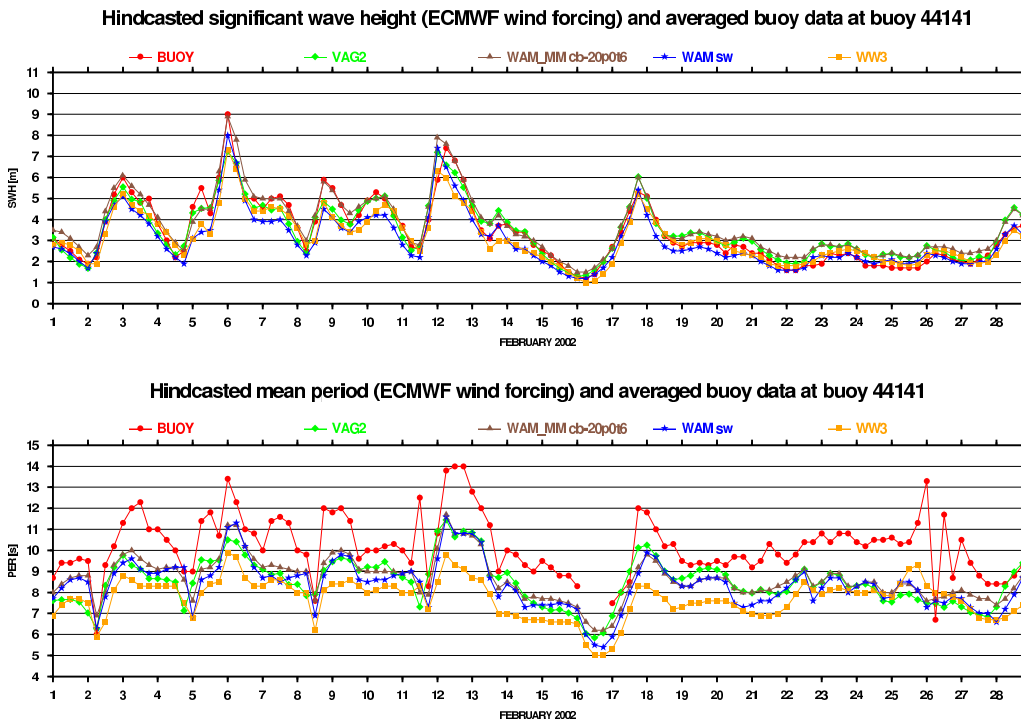


Figure 10: Time series of swh and mean (for the models) or peak (for the buoy) period at buoy 44141 for February 2002

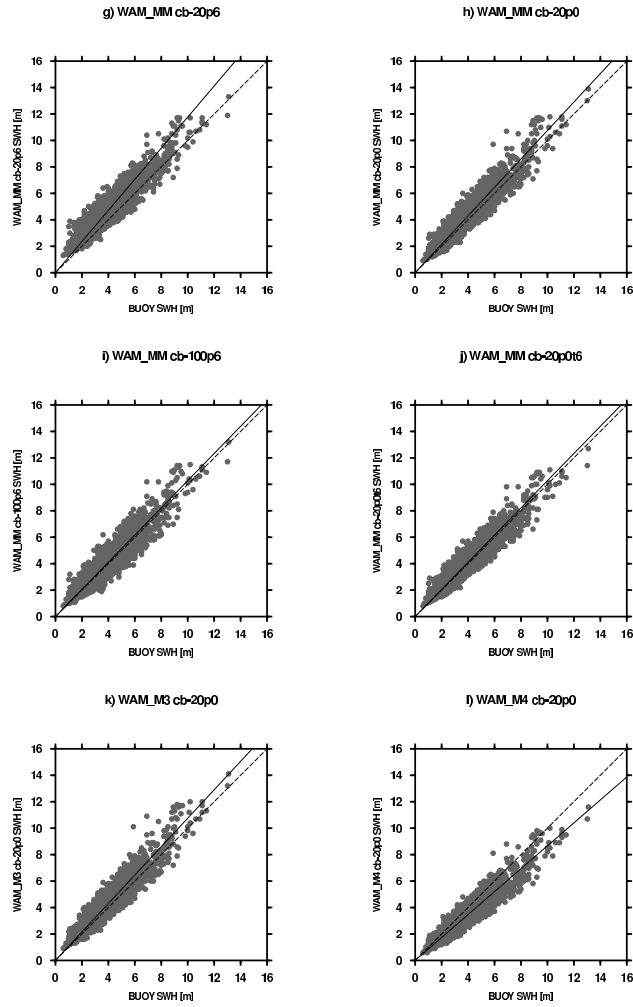


Figure 11: Comparisons model wave heights with averaged buoy data for february 2002

| Model          | ECMWF | VAG2 dw | WAM dw | WW3 dw |
|----------------|-------|---------|--------|--------|
| No. of entries | 2490  | 2490    | 2490   | 2490   |
| Buoy mean      | 8.87  | 3.69    | 3.69   | 3.69   |
| Bias           | 0.61  | -0.26   | -0.46  | -0.24  |
| Rms error      | 1.74  | 0.74    | 0.74   | 0.67   |
| Scatter index  | 0.18  | 0.19    | 0.16   | 0.17   |
| Symm. slope    | 1.08  | 0.92    | 0.87   | 0.94   |

Table 2: Wind speed and swh statistics for February 2002

| Model          | WAM sw | WAM_MM sw<br>(cb-20 p6) | WAM_MM sw<br>(cb-20 p0) | WAM_MM sw<br>(cb-100 p6) | WAM_MM sw<br>(cb-20 p0t6) | WAM_M3 sw<br>(cb-20 p0) | WAM_M4 sw<br>(cb-20 p0) |
|----------------|--------|-------------------------|-------------------------|--------------------------|---------------------------|-------------------------|-------------------------|
| No. of entries | 2490   | 2490                    | 2490                    | 2490                     | 2490                      | 2490                    | 2490                    |
| Buoy mean      | 3.69   | 3.69                    | 3.69                    | 3.69                     | 3.69                      | 3.69                    | 3.69                    |
| Bias           | -0.48  | 0.79                    | 0.32                    | 0.09                     | 0.16                      | 0.30                    | -0.49                   |
| Rms error      | 0.75   | 0.99                    | 0.65                    | 0.64                     | 0.57                      | 0.65                    | 0.75                    |
| Scatter index  | 0.16   | 0.16                    | 0.15                    | 0.17                     | 0.15                      | 0.16                    | 0.15                    |
| Symm. slope    | 0.87   | 1.18                    | 1.07                    | 1.03                     | 1.03                      | 1.07                    | 0.87                    |

Table 3: Swh statistics for February 2002

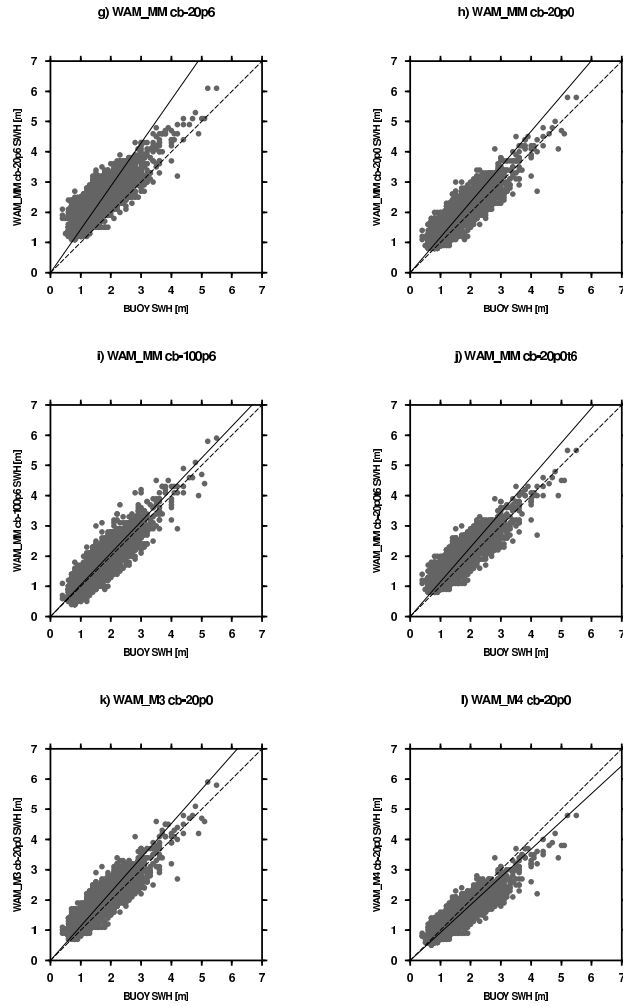


Figure 12: Comparisons model wave heights with averaged buoy data for July 2002

| Model          | ECMWF | VAG2 dw | WAM dw | WW3 dw |
|----------------|-------|---------|--------|--------|
| No. of entries | 2398  | 3316    | 3316   | 3316   |
| Buoy mean      | 6.19  | 1.68    | 1.68   | 1.68   |
| Bias           | 0.12  | 0.08    | -0.02  | -0.07  |
| Rms error      | 1.08  | 0.36    | 0.34   | 0.31   |
| Scatter index  | 0.17  | 0.21    | 0.20   | 0.18   |
| Symm. slope    | 1.02  | 1.02    | 0.97   | 0.96   |

Table 4: Wind speed and swh statistics for July 2002

| Model          | WAM sw | WAM_MM sw<br>(cb-20 p6) | WAM_MM sw<br>(cb-20 p0) | WAM_MM sw<br>(cb-100 p6) | WAM_MM sw<br>(cb-20 p0t6) | WAM_M3 sw<br>(cb-20 p0) | WAM_M4 sw<br>(cb-20 p0) |
|----------------|--------|-------------------------|-------------------------|--------------------------|---------------------------|-------------------------|-------------------------|
| No. of entries | 3316   | 3316                    | 3316                    | 3316                     | 3316                      | 3316                    | 3316                    |
| Buoy mean      | 1.68   | 1.68                    | 1.68                    | 1.68                     | 1.68                      | 1.68                    | 1.68                    |
| Bias           | -0.05  | 0.81                    | 0.33                    | 0.08                     | 0.30                      | 0.26                    | -0.11                   |
| Rms error      | 0.33   | 0.89                    | 0.45                    | 0.33                     | 0.43                      | 0.39                    | 0.31                    |
| Scatter index  | 0.20   | 0.23                    | 0.19                    | 0.19                     | 0.19                      | 0.17                    | 0.18                    |
| Symm. slope    | 0.95   | 1.43                    | 1.17                    | 1.05                     | 1.15                      | 1.13                    | 0.92                    |

Table 5: Swh statistics for July 2002

## 5. CONCLUSION AND PERSPECTIVES

A new parameterization of the sea drag as well as new formulations of wind input and dissipation source terms have been implemented in the WAM cycle 4 model and tested on a global grid. Different configurations of the WAM model have been investigated, depending on the wind input and dissipation formulations and the value of some coefficients used in the wind input and dissipation source terms. Improvements in swell dissipation have been found for *WAM\_MMcb - 20p0* and *WAM\_MMcb - 20p0t6* configurations. The new formulations of sea drag and wind input and dissipation source terms introduced in the WAM model resulted in a better prediction of swh in many cases and reductions in bias and rms error of this parameter. The global statistics computed for February 2002 showed the best quality for *WAM\_MMcb-20p0t6* configuration, compared to the other configurations of WAM and also VAG and WW3 models. For July 2002, *WAM\_MMcb - 100p6* and WW3 gave the best prediction of swh, while *WAM\_MMcb-20p0t6* overestimated the values of of this parameter.

The results obtained with the new physical parameterizations introduced in WAM are very encouraging. Further experiments can be done in order to adjust the coefficients for a better balance of the new physical parameterizations.

## REFERENCES

Alves J. H. G. M., Banner M. L., 2003: Performance of a Saturation-Based Dissipation-Rate Source Term in Modeling the Fetch-Limited Evolution of Wind Wave s. *Journal of Physical Oceanography*, Vol. 33, No. 6, pp. 1274-1298.

Banner M. L. and Young I. R., 1994: Modelling spectral dissipation in the evolution of wind waves. Part1: assessment of existing model performance. *J. Phys. Oceanogr.*, 24, pp. 1550-1570.

Courtier P., Freydier C., Geleyn J-F., Rabier F. and Rochas M., 1991: The ARPEGE project at Meteo-France. In ECMWF 1991 Seminar Proceedings: Numerical methods in atmospheric models; ECMWF, 9 - 13 September 1991, Vol. II, pp. 193-231.

Fradon B., 1997: Modelisation numerique de l'etat de la mer: comparaison des performances et de limites d'un modele de deuxieme generation et de'un modele de troisieme generation dans le cadre de l'experience SEMAPHORE. These de doctorat de l'Universite Paris VII.

Fradon B., Hauser D., Lefevre J-M., 1999: Comparison Study of a Second-Generation and of a Third-Generation Wave Prediction Model in The Context of the S EMAPHORE Experiment. *J. of Atmosph. and Oceanogr. Tech.* (2000), 17, pp. 197-214.

Guillaume A., 1987: VAG-Modele de prevision de l'etat de la mer en eau profonde. Note de travail de l'Etablissement d'Etudes et de Recherches Meteorologiques, No 178.

Günther H., Hasselmann S., Janssen P.A.E.M., 1992: The WAM model Cycle 4.0. User Manual, Deutsches Klima Rechen Zentrum, Technical Report No. 4.

Hasselmann K., 1974: On the spectral dissipation of ocean waves due to whitecapping. *Boundary-Layer Meteorology*, 6, pp. 107-127.

Janssen P.A.E.M., 1989: Wave-Induced Stress and the Drag of Air Flow over Sea Waves. *Journal of Physical Oceanography*, 19, pp. 745-754.

Janssen P.A.E.M., 1991: Quasi-linear Theory of Wind-Wave Generation Applied to Wave Forecasting. *Journal of Physical Oceanography*, 21, pp. 1631-1642.

Komen G. J., Cavaleri L., Donelan M., Hasselmann K., Hasselmann S., Janssen P. A. E. M., 1994: Dynamics and modelling of ocean waves. Cambridge University Press, 532 pp.

Kudryavtsev V. N., Makin V. K. and Chapron B., 1999: Coupled sea surface-atmosphere model 2. Spectrum of short wind waves. *J. of Geophys. Res.*, 104, pp. 7 625-7639.

Kudryavtsev V. N., Makin V. K., 2001: The impact of air-flow separation on the drag of the sea surface. *Boundary-Layer Meteorology*, 98, pp. 155-171.

Lefevre J-M., Kortcheva A., Stefanescu S., 2003: Performance of Several Wave Forecasting Systems for High Swell Conditions. The Proceedings of The Thirteenth (2003) International Offshore and Polar Engineering Conference, Vol. III, pp. 117-122.

Makin V. K., Kudryavtsev V. N. and Mastenbroek C., 1995: Drag of the sea surface. *Boundary-Layer Meteorology*, 79, pp. 159-182.

Makin V. K. and Kudryavtsev V. N., 1999: Coupled sea surface-atmosphere model 1. Wind over waves coupling. *J. of Geophys. Res.*, 104, pp. 7613-7623.

Makin V. K. and Kudryavtsev V. N., 2002: Impact of dominant waves on sea drag. *Boundary-Layer Meteorology*, 103, pp. 83-99.

Makin V. K., 2003: A note on a parameterization of the sea drag. *Boundary-Layer Meteorology*, 106, pp. 593-600.

- Makin V. K. and Stam M., 2003: New drag formulation in NEDWAM. Technical Report of KNMI no. 250.
- Miles J. W., 1957: On the generation of surface waves by shear flows. *J. Fluid. Mech.*, 3, pp. 185-204.
- Miles J. W., 1959: On the generation of surface waves by shear flows. Part 2. *J. Fluid. Mech.*, 6, pp. 568-582.
- Simmons A. J., Burridge D. M., Jarraud M., Girard C. and Wergen W., 1989: The ECMWF medium-range prediction models development of the numerical formulations and the impact of increased resolution. *Meteorol. Atmos. Phys.*, 40, pp. 28-60.
- Stefanescu S., Lefevre J-M., 2001: Implementation of new physics in the operational version of the wave model VAG. Internal Report of Division Marine and Oceanography, Meteo-France.
- Stefanescu S., Lefevre J-M., Kortcheva A., Makin V., 2004: Recent developments in physical parametrizations used in VAG and WAM wave models. Presentation to the Black Sea Coastal Air-Sea Interactions/Phenomena and elated Impacts and Applications International Workshop, 13-15 May 2004, Constanta, Romania.
- Tolman, H. L., 2002: User manual and system documentation of WAVEWATCH-III version 2.22. NOAA / NWS / NCEP / OMB Technical Note NR. 222, 133 pp.
- WAMDIG, 1988: The WAM model - A third generation ocean wave prediction model. *Journal of Physical Oceanography*, 18, pp. 1775-1810.